INORGANIC CHEMISTRY

FRONTIERS

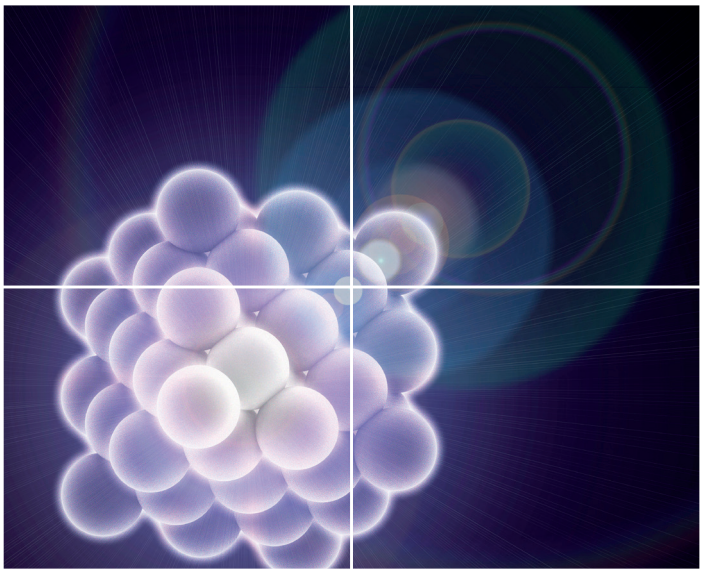

Accepted Manuscript

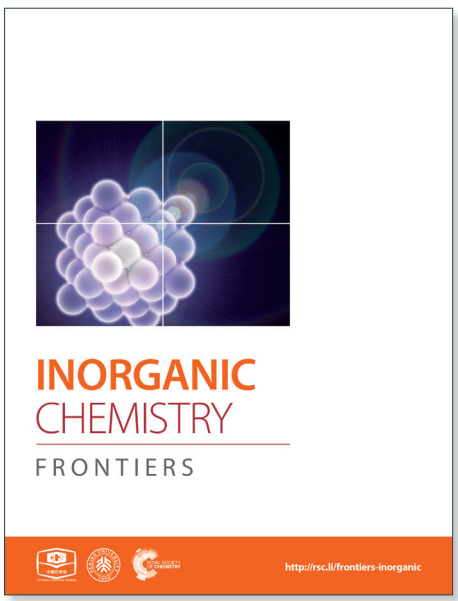

This is an *Accepted Manuscript*, which has been through the Royal Society of Chemistry peer review process and has been accepted for publication.

Accepted Manuscripts are published online shortly after acceptance, before technical editing, formatting and proof reading. Using this free service, authors can make their results available to the community, in citable form, before we publish the edited article. We will replace this *Accepted Manuscript* with the edited and formatted *Advance Article* as soon as it is available.

You can find more information about *Accepted Manuscripts* in the **Information for Authors**.

Please note that technical editing may introduce minor changes to the text and/or graphics, which may alter content. The journal's standard **Terms & Conditions** and the **Ethical guidelines** still apply. In no event shall the Royal Society of Chemistry be held responsible for any errors or omissions in this *Accepted Manuscript* or any consequences arising from the use of any information it contains.

Journal Name

RSCPublishing

ARTICLE

Removal of CO_2 from CH_4 and CO_2 Capture in the Presence of H_2O Vapour in NOTT-401

Cite this: DOI: 10.1039/x0xx00000x

Hugo A. Lara-García, Maximiliano R. Gonzalez, Juan H. González-Estefan, Pedro Sánchez-Camacho, Enrique Lima, and Ilich A. Ibarra*

Received 00th January 2012,
Accepted 00th January 2012

DOI: 10.1039/x0xx00000x

www.rsc.org/

From a binary equimolar gas-mixture of CO_2 and CH_4, NOTT-401 exhibits CO_2 separation from CH_4. By kinetic uptake experiments, NOTT-401 confirms a maximum of 1.47 wt% CO_2 capture at 30 ^oC and a significant 7-fold increase (~9.90 wt%) in CO_2 capture under 40% relative humidity of water vapour.

Introduction

The use of natural gas as fuel is indeed, very advantageous for the environment and it is also economically attractive. If natural gas is used as a vehicular fuel, the reductions in CO, SO_2 and CO_2 are 97, 90 and 24 %, respectively, and there is not lead release in exhaust gases. Additionally, it is cheaper than gasoline or diesel. To date, natural gas supplies one-fourth of the energy needed in homes, factories, business, vehicles, industries and power plants around the world. It is estimated that the consumption of natural gas will grow by 50 % over the next 10 years.[1-2] The main constituent of natural gas is methane (CH_4), which has the highest hydrogen to carbon (H/C) ratio of all hydrocarbon fuels.[3] However, the quality of natural gas, coming from land fields and biogas plants, is considerably low with impurities like CO_2 (20 to 35%), N_2, H_2O and H_2S.[4] Then, pre-combustion CO_2 sequestration from natural gas is essential to maximize its energy content (CH_4). Additionally, post-combustion CO_2 capture from plant flue gas is also crucial in order to control greenhouse emissions.[5]

CO_2 directly affects our environment by causing raising of global temperature and acidification of the oceans.[6] The main source of the increasing CO_2 levels is the accelerating global energy demands.[7] These energy requirements are expanding promptly due to rapid world population growth, increases in standard of living and the development of technologies leading to a doubling in the energy demand over the last three decades.[8] Thus, CO_2 separation and capture have extremely motivated many governments to invest in the development of new methods for efficiently and effectively capturing CO_2.[9] Typical absorption in aqueous alkanolamine solutions has been widely used and studied, but it has many major limitations as an adsorbent for industrial CO_2 capture due to its heat instability and corrosion towards vessels and pipelines.[10] Therefore, the use of porous solids for the adsorption of CO_2 is a timely research area and the seek for materials with a high adsorption capacity, structural stability, fast sorption kinetics and mild regeneration properties, remains a major challenge.

Porous coordination polymers (PCPs) or metal-organic frameworks (MOFs) are among the most promising candidates for gas separation, because their sorption selectivity towards small molecule adsorbates is directly tunable as a function of the topology and chemical composition of the micropores.[11] Porous metal-organic materials showing high surface area and high pore volume normally show high CO_2 storage capacities at room temperature and relatively high pressures.[12] Although the high CO_2 capacity and selectivity that PCPs show, many gas separation processes involve the exposure to water vapor.

However, a small number of PCPs have shown good stability to water, and water is most often unfavorable to gas separations.[13] Along with those few examples, Hong *et al*.[14] reported a water-stable PCP based on a binuclear [$In_2(\mu_2$-OH)] building block (see Scheme S1, ESI†), InOF-1, constructed from a flexible $BPTC^{4-}$ ligand (H_4BPTC= biphenyl-3,3',5,5'-tetracarboxylic acid) which also showed a high CO_2/N_2 and CO_2/CH_4 selectivities (by using the experimental single-component gas adsorption isotherms). The effect of water on the CO_2 capture has only recently been investigated on PCPs.[15] Matzger and co-workers[15b] studied the effect of humidity on the performance of M/DOBDC (M = Zn^{II}, Ni^{II}, Co^{II} or Mg^{II}) by collecting $N_2/CO_2/H_2O$ breakthrough curves at different relative humidities. LeVan *et al*.[16] found that a small amount of water did not decrease and may actually increase the CO_2 capacity of PCPs.

Interestingly, Llewellyn and co-workers[17] investigated the CO_2 adsorption in some PCPs under different relative

Inorganic Chemistry Frontiers Accepted Manuscript

humidities of water vapour. Indeed, HKUST-1, was shown to degrade in the presence of humidity, and UiO-66 did not show any enhanced CO_2 uptake.[17] In the case of MIL-100(Fe), a remarkable 5-fold increase in CO_2 uptake was observed with increasing relative humidity (RH), 105 mg g^{-1} at 40% RH. In addition, Yaghi *et al.*[18] showed that the presence of hydroxyl functional groups increase the affinity of the framework for water. Thus, in the present work we have chosen a material entitled NOTT-401[19] (Fig.1) based on a binuclear [$Sc_2(\mu_2$-OH)] building block (see Scheme S1, ESI†) which is the same building block to the water-stable InOF-1[14] and possesses hydroxo functional groups (μ_2-OH) to study the separation of a binary gas mixture (not a single-component gas) of CO_2 and CH_4 and we have successfully performed CO_2 capture in the presence of water vapour.

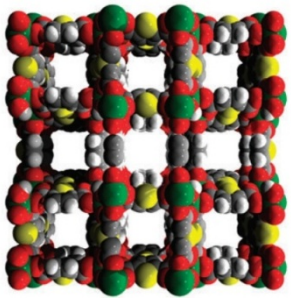

Fig. 1 Space-filling view of the structure of NOTT-401 along the *c*-axis (scandium: green; sulphur: yellow; oxygen: red; carbon: grey; hydrogen: small grey).[19]

Experimental

Scandium triflate (0.057 g, 0.116 mmol) and thiophene-2,6-dicarboxylic acid, H_2TDA, (0.01 g, 0.058 mmol) were dispersed in THF (4.0 ml), DMF (3.0 ml), H_2O (1.0 ml) and HCl (36.5 %, 2 drops) and sealed in a pressure tube. The clear solution was heated at 90 ^oC in an oil bath for 72 h. The tube was cooled to room temperature over a period of 12 h and the colorless crystalline product separated by filtration, washed with DMF (5.00 ml) and dried in air. Yield: 71.1 % (based on ligand).

The uncoordinated solvent molecules in the pores of the as-synthesized NOTT-401 were exchanged for acetone and this promotes accessibility to the desolvated framework after activation by heating. Thus, thermogravimetric (See Fig. S1, ESI†) analysis and bulk powder x-ray diffraction patterns (See Fig. S2, ESI†) of as-synthesised and desolvated NOTT-401 confirmed that the material consistently retains its structural integrity upon solvent removal. N_2 adsorption isotherms for activated NOTT-401[19] at 77 K were used to calculate the BET surface area ($0.01<p/p_o<0.04$) of 1514 m^2 g^{-1}.

A catalytic reactor system (BEL-REA, BEL Japan; See Fig. S3, ESI†) was employed to evaluate the separation of CO_2 from CH_4. This catalytic reactor system allowed each sample of acetone-exchanged NOTT-401 to be activated (150 ^oC for 2h) under a flow of N_2 gas and then directly exposed to adsorbates (CO_2 and CH_4) in situ, and studied by FTIR spectroscopy over many cycles without physical manipulation or exposure to air.

Kinetic uptake experiments were performed by using a thermobalance (Q500 HR, from TA) at different temperatures with a constant CO_2 flow (60 mL min^{-1}). Then, acetone-exchanged samples of NOTT-401 were placed into the thermobalance and activated by heating from room temperature to 150 ^oC for 2h and under a flow of N_2 gas. After the activated sample was cooled down, the desired temperature was set and a constant CO_2 flow (60 mL min^{-1}) was started. With a humidity-controlled thermobalance (Q5000 SA, from TA) kinetic uptake experiment at 30 ^oC with a constant CO_2 flow (60 mL min^{-1}) we carried out on activated samples (150 ^oC for 2h and under a flow of N_2 gas) of NOTT-401.

Results

An acetone-exchanged sample of NOTT-401 (40 mg) was packed into the holder sample in the BEL-REA system (See Fig. S3, ESI†) and activated as described before (*vide supra*). Then, the system was allowed to cool down to room temperature (30 ^oC) and the activated NOTT-401 sample was exposed to a flow of the binary equimolar (0.13 mmol min^{-1}) gas mixture of CO_2 and CH_4. This mixture corresponds to a more realistic composition in the field of gas-separation processes. Then, after stabilization of the gas flow within the sample, the resulting exit exhaust gases were analysed by FTIR spectroscopy (see Fig. S3, ESI†). Each FTIR spectrum was recorded every 40 seconds (~0.66 min), until the detector was saturated, to make a sum of 10 FTIR spectra (see Fig. S4, ESI†).

The most characteristic FTIR bands for the CO_2 and CH_4 molecules are at 2349 cm^{-1} and 3016 cm^{-1}, respectively, Fig. 2. In both cases, it is possible to monitor a continuous increase in the characteristic band intensities (Fig. 2), for CO_2 and CH_4 in time. Therefore, from spectrum 1 to spectrum 10 the intensity of the characteristic FTIR band is increasing while the transmittance is decreasing.

Inorganic Chemistry Frontiers Accepted Manuscript

This journal is © The Royal Society of Chemistry 2012

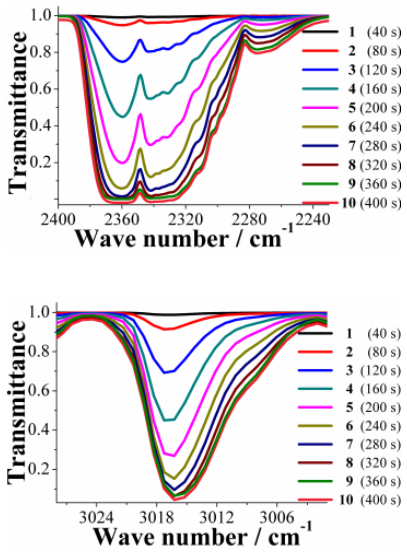

Fig. 2 FTIR spectra of the resulting exit exhaust of the binary equimolar (0.13 mmol min^{-1}) gas-mixture of CO_2 and CH_4 of: (top); the characteristic CO_2 band and (bottom); the characteristic CH_4 band.

The intensities of these characteristic CO_2 and CH_4 FTIR bands demonstrated to be different. This could suggest that the CO_2 and CH_4 molecules arrive at the FTIR detector with different times. By normalizing the intensities, considering their respectively transmittances, it is possible to plot the increase in intensity of each scan for CO_2 and CH_4 simultaneously (Fig. 3, top). The normalized intensity, for each scan, of CH_4 is higher than CO_2, suggesting that the molecules of CH_4 effectively arrive at the FTIR detector before the CO_2 molecules. It is possible to rationalize this result as follows; when the binary gas mixture (CO_2 and CH_4) goes through the activated sample NOTT-401 this material retains CO_2 stronger than CH_4, and therefore, the CH_4 gas molecules flow 'faster' inside the material and are detected earlier. To verify this hypothesis, we carried out three more experiments: first, an acetone-exchanged sample of NOTT-401 (40 mg) was packed into the BEL-REA system, activated and stabilized as described (see below) and a flow of only CO_2 (0.13 mmol min^{-1}) was set. Then, the exit exhaust gas was analyzed by FTIR spectroscopy and 10 scans were collected, until the detector was saturated (see Fig. S5, ESI†).

Second, another acetone-exchanged NOTT-401 (40 mg) sample was packed in the BEL-REA system, activated, stabilized and analyzed as described before. Then, the sample was exposed to a flow of only CH_4 gas (0.13 mmol min^{-1}). As in the previous experiment, 10 FTIR spectra were recorded from the exit exhaust gas until the detector was saturated (see Fig. S6, ESI†). Again, by normalizing the characteristic FTIR intensities it was possible to simultaneously plot the normalized intensity of each scan for CO_2 and CH_4 (Fig. 3, bottom).

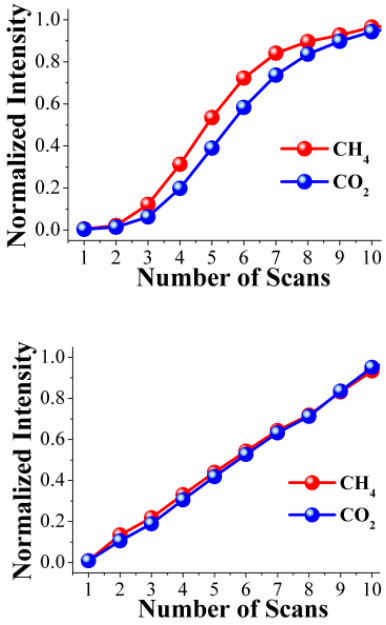

Fig. 3 Normalized characteristic FTIR intensities of CO_2 and CH_4 as a function of the number of scans. (top) FTIR intensities from a resulting exit exhaust of the binary equimolar (0.13 mmol min^{-1}) gas-mixture of CO_2 and CH_4; (bottom) FTIR intensities from individual flows of CO_2 and CH_4.

The normalized intensities for CO_2 and CH_4 at each scan (from 1 to 10) are basically the same (Fig. 3, bottom) suggesting that when the resulting exit exhaust of each pure-gas component (not a gas mixture) is analyzed separately by FTIR spectroscopy, the molecules of CO_2 and CH_4 arrive at the same time to the FTIR detector. These results corroborate that NOTT-401 is more selective to CO_2 than CH_4 when a binary equimolar (0.13 mmol min^{-1}) gas-mixture of CO_2 and CH_4 travels within an activated sample. We interpreted this selectivity as the time delay of the CO_2 molecules in reaching the FTIR detector. By polynomial regressions of the normalized intensities on Fig. 3 (top), we estimated this delay to be ~ 23 s (see Fig. S7 and S8 ESI†).

Finally a third last-experiment was carried out: in order to confirm that this delay was due to the adsorption selectivity showed by NOTT-401 (a microporous PCP) rather than other phenomena, a non-porous material (PCM-14[20]) was packed in the BEL-REA system. PCM-14 is a dense coordination polymer that has shown to be a non-porous material when it is activated between 25-150 °C. Then, a sample of PCM-14 (40 mg) was activated at 150 °C for 2h under a flow of N_2 gas and then directly exposed to binary equimolar (0.13 mmol min^{-1}) CO_2 and CH_4 gas mixture. The resulting exit exhaust gas was analyzed by FTIR spectroscopy and just 6 scans were recorded, until the detector was saturated. By normalisation of the characteristic FTIR intensities, we plotted the normalized intensities of each CO_2 and CH_4 scans (see Fig. S9, ESI†). Interestingly, the normalized intensities for CO_2 and CH_4 at each scan (from 1 to 6) are essentially the same (see Fig. S9,

Inorganic Chemistry Frontiers Accepted Manuscript

ESI†) corroborating that the time delay is due to the microporosity of NOTT-401.

Dynamic and isothermal CO_2 experiments were carried out on NOTT-401. Fig. 4, top, shows the kinetic uptake experiments from 30 °C to 100 °C. At 30 °C the material exhibited the maximum weight % gain, which represents the maximum amount of CO_2 captured. This amount corresponds to 1.47 wt% and it was rapidly reached (constant uptake) after just ~300 s (5 min) and it kept constant until the end of the experiment (3600 s or 60 min). At 40 °C the uptake was estimated to be 1.16 wt% and it was also reached after around 300 s (Fig. 4, top). Clearly, while the temperature is increased (from 30 to 100 °C), the CO_2 weight (%) gradually decreases (Fig. 4, top) to 0.09 wt% (at 100 °C) and interestingly, the kinetic uptake experiments did not show any difference in the equilibrium times. These equilibrium times have been previously observed in another microporous material entitled NOTT-400.[21]

In order to corroborate that this decrease is not due to sample degradation, we have carried out PXRD experiments on each sample after these CO_2 capture experiments. Fig. 4 (bottom) confirms that the crystallinity of the samples after each CO_2 capture experiments was retained.

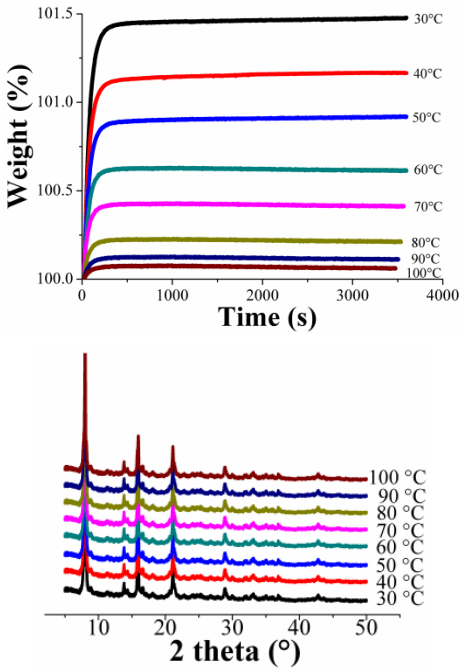

Fig. 4 (top) Kinetic uptake experiments performed at different temperatures (30, 40, 50, 60, 70, 80, 90 y 100 °C) with a CO_2 flow of 60 mL/min; (bottom) PXRD patterns of each NOTT-401 samples after the kinetic CO_2 isotherms were carried out at different temperatures.

Encouraged by the promising results that Hong *et al.* reported,[14] by showing a water stable framework (InOF-1) with the same binuclear [$M_2(\mu_2$-OH)] building block to NOTT-401, we explored the water stability of NOTT-401. Then, acetone-exchanged samples of NOTT-401 were exposed to air and soaked in distilled water. PXRD patterns of these samples (see Fig. S10, ESI†) confirmed structural stability of NOTT-401 in water. In addition, we calculated the BET surface areas (by N_2 adsorption isotherms, $0.01<p/p_o<0.04$) of samples NOTT-401 exposed to air and NOTT-401 soaked in distilled water of 1510 and 1516 $m^2\ g^{-1}$, respectively. This demonstrates that NOTT-401 retains its surface area after water exposure.

This water-stability can be attributed to the presence of the hydroxo functional groups (inside the pores of NOTT-401) which has been previously shown[19] and these functional groups, increase the affinity of the material for water. Indeed, Walton *et al.*[22] proposed that the functional groups act as a directing agent for water in the pores, which can allow for more efficient packing. Thus, after founding the best CO_2 capture temperature (30 °C, Fig.4, top), under anhydrous conditions, a kinetic isotherm experiment at 30 °C, with a constant CO_2 flow, and a relative humidity (RH) of 40% was carried out. It was decided to run this experiment with a 40% RH based on the remarkable results that Llewellyn *et al.*[17] previously reported (5-fold increase in CO_2 uptake for MIL-100(Fe)). An activated NOTT-401 sample (150 °C for 2h and under a flow of N_2 gas) was placed into a humidity-controlled thermobalance. After activation of the material, the equipment was stabilized at 40% RH (30 °C) and a constant CO_2 flow (60 mL min^{-1}) was started. Afterwards, we repeated this experimental procedure on a new activated NOTT-401 sample and set a constant N_2 flow (60 mL min^{-1}). Fig. 5 exhibits the kinetic uptake experiments at 30 °C and 40% RH for CO_2 and N_2. For both isotherms, it is clear to observe that the material shows a constant increase in weight (while the experiment is continuing in time, see Fig. 5). This increase in weight is due to the contribution of H_2O and CO_2 or H_2O and N_2, respectively.

In order to find the maximum CO_2 capture under 40% RH conditions, we need to differentiate the contribution of H_2O to the weight increase. By just taking the difference of the two isotherms (CO_2 and N_2) we could obtain the CO_2 capture at 40% RH. This is valid if the material does not capture any N_2 at 30 °C. Consequently, by performing a kinetic uptake experiment on a new activated NOTT-401 sample at 30 °C without any presence of H_2O vapor (0% RH) with a constant N_2 flow (60 mL min^{-1}) we obtained a N_2 capture of approximately 0.01 wt%. This result is consistent with previous reports where the capture capacity of N_2 capture in PCPs at room temperatures is basically negligible.[23] In Fig. 5, the gradual weight increase (for CO_2/H_2O and N_2/H_2O) starts at 0 s and stabilises at ~ 7000 s (117 min). In contrast, under anhydrous conditions the CO_2 uptake rapidly reached stability (5 min, see Fig. 4, top). This equilibrium discrepancy is due to the nature of the vapour adsorption process that in general takes considerably more time to reach stability than the gas adsorption process in microporous materials.[24] Then, from 7000 s until approximately 8700 s (145 min) both isotherms seem to reach a plateau where both uptakes are practically constant (Fig. 5, red rectangle). At 8700 s, the maximum amounts of CO_2/H_2O and N_2/H_2O captured are 12.60 wt% and 2.70 wt%, respectively and by simply taking the difference of these two values (since there is

Inorganic Chemistry Frontiers Accepted Manuscript

This journal is © The Royal Society of Chemistry 2012

no N_2 uptake at 30 °C) the CO_2 capture in the materials is ~ 9.90 wt%. Finally, from 8700 s to 11000 s (Fig. 5) the flow of each gas and the relative humidity were stopped and the decrease in weight represents the gas and water vapour desorption.

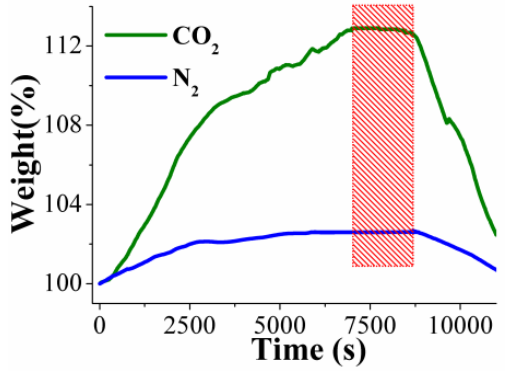

Fig. 5 Kinetic uptake experiments carried out at 30 °C and 40% RH with CO_2 (green line) and N_2 (blue line) flows of 60 mL/min, respectively.

Therefore, the CO_2 capture was approximately 7-fold increased with a 40% RH. This enhance in CO_2 uptake in the presence of water can be explained by CO_2 confinements effects induced by bulky molecules (H_2O).[25] In addition, we decided to carry a CO_2 experiment out (60 mL min^{-1}) at 40% RH and 30 °C on an activated PCM-14[20] sample (150 °C for 2h, under a flow of N_2 gas). Since PCM-14 is a non-porous coordination polymer, when activated between 25-150 °C, it offered a direct CO_2 capture comparison to NOTT-401 (microporous material). Thus, from 0 s to 11000 s the maximum CO_2 uptake (under 40% RH) was 0.8 wt% (see Fig. S11, ESI†). This result corroborated that there is no CO_2 sequestration in a non-porous material when the relative humidity is 40% at 30 °C.

Conclusions

In conclusion, NOTT-401, a Sc(III) porous coordination polymer, exhibited CO_2 separation from CH_4, in a more realistic scenario, when this microporous material was exposed to a binary, CO_2/CH_4, equimolar gas-mixture. By running these equimolar (CO_2/CH_4) gas experiments on PCM-14, a non-porous coordination polymer, it was established that the intrinsic microporosity of NOTT-401 is responsible for the gas separation.

By kinetic isotherm experiments, NOTT-401 exhibits a total CO_2 amount of 1.47 wt% at 30 °C, which was rapidly reached after just approximately 300 s. While increasing the temperature of the kinetic isotherm experiments, the CO_2 capture capacity of NOTT-401 decreased considerably to less than 0.1 wt% at 100 °C. Remarkably, NOTT-401 exhibits high stability towards humidity, which was corroborated by PXRD. We attributed this water stability, as previously reported,[18,22] to the presence of hydroxo functional groups within the pores of NOTT-401. Due to this particularly high water stability, NOTT-401 performs CO_2 uptake under relative humidity conditions (40% RH) and 30 °C, displaying a maximum CO_2 capture of approximately 9.9 wt%.

Significantly, this CO_2 capture, under humid conditions, represents a 7-fold increase in comparison to anhydrous conditions. PCM-14 showed non CO_2 capture under RH conditions, suggesting that the microporosity provided by NOTT-401 is fundamental for this capture process. Since PCM-14 is non-porous coordination polymer, when activated between 25-150 °C, the CO_2 confinement effects induced by H_2O[25] in porous materials cannot take place unlike NOTT-401 where these effects occur within the micropores.

Acknowledgements

The authors thank Dr. A. Tejeda-Cruz (X-ray; IIM-UNAM), CONACyT Mexico (212318), PAPIIT UNAM Mexico (IN100415) for financial support. M.R.G. thanks CONICET and BECAR Argentina for scholarship funding. Thanks to U. Winnberg (ITAM) for scientific discussions.

Notes and references

Instituto de Investigaciones en Materiales, Universidad Nacional Autónoma de México, Circuito Exterior s/n, CU, Del. Coyoacán, 04510, México D. F., Mexico.

Electronic Supplementary Information (ESI) available: TGA data, PXRDP data, FTIR data, Polynomial Regressions and Kinetic Uptake Experiments. See DOI: 10.1039/b000000x/

1 F. W. Lipfert, *Air Pollution and Community Healt: A Critical Review and Data Source Book*, Van Nostrand Reinhold, New York, USA, 1994, p. 556.
2 P. D. Noyes, M. K. McElwee, H. D. Miller, B. W. Clark, L. A. Van Tiem, K. C. Walcott, K. N. Erwin and E. D. Levin, *Environ. Int.*, 2010, **35**, 971.
3 T. Burchell, M. Rogers, *SAE Tech. Pap. Ser.*, 2000, 2000.
4 M. Herout, J. Malat'ák, L. Kučera and T. Dlabaja, *Res. Agric. Eng.*, 2011, **57**, 137.
5 D. M. D'Alessandro, B. Smit and J. R. Long, *Angew. Chem., Int. Ed.*, 2010, **49**, 6058.
6 J. T. Litynski, S.M. Klara, H. G.McIlvried and R. D. Srivastava, *Environ. Int.*, 2006, **32**, 128.
7 M. Z. Jacobson, *Energy Environ. Sci.*, 2009, **2**, 148.
8 International Energy Agency (IEA), Key World Energy Statistics, OECD/IEA, France, 2013.
9 K. Sumida, D. L. Rogow, J. A. Mason, T. M. McDonald, E. D. Bloch, Z. R. Herm, Z. T.-H. Bae and J. R. Long, *Chem. Rev.*, 2012, **112**, 724.
10 (a) G. T. Rochelle, Science, 2009, **325**, 1652; (b) F. Karadas, M. Atilhan and S. Aparicio, Energy Fuels, 2010, **24**, 5817.

Inorganic Chemistry Frontiers Accepted Manuscript

11 (a) S. Yang, G. S. B. Martin, G. J. J. Titman, A. J. Blake, D. R. Allan, N. R. Champness and M. Schröder, *Inorg. Chem.*, 2011, **50**, 9374; (b) A. J. Nuñez, L. N. Shear, N. Dahal, I. A. Ibarra, J. W. Yoon, Y. K. Hwang, J.-S. Chang and S. M. Humphrey, *Chem. Commun.*, 2011, **47**, 11855.

12 (a) H. Furukawa, N. Ko, Y. B. Go, N. Aratani, S. B. Choi, E. Choi, A. Ö. Yazaydin, R. Q. Snurr, M. O'Keeffe, J. Kim and O. M. Yaghi, *Science*, 2010, **329**, 424; (b) A. M. Bohnsack, I. A. Ibarra, P. W. Hatfield, J. W. Yoon, Y. K. Hwang, J.-S. Chang and S. M Humphrey, *Chem. Commun.*, 2011, **47**, 4899; (c) P. Nugent, Y. Belmabkhout, S. D. Burd, A. J. Cairns, R. Luebke, K. Forrest, T. Pham, S. Ma, B. Space, L. Wojtas, M. Eddaoudi and M. J. Zaworotko, *Nature*, 2013, **495**, 80.

13 (a) S. S. Nagarkar, A. K. Chaudhari and S. K. Ghosh, Inorg. Chem., 2012, **51**, 572; (b) H. J. Choi, M. Dincă, A. Daily and J. R. Long, *Energy Environ. Sci.*, 2010, **3**, 117.

14 J. Qian, F. Jiang, D. Yuan, M. Wu, S. Zhang, L. Zhang and M. Hong, *Chem. Commun.*, 2012, **48**, 9696.

15 (a) J. Liu, A. I. Benin, A. M. B. Furtado, P. Jakubczak, R. R. Willis and M. D. LeVan, *Langmuir*, 2011, **27**, 11451; (b) A. C. Kizzie, A. G. Wong-Foy and A. J. Matzger, *Langmuir*, 2011, **27**, 6368; (c) H. Jasuja, Y.-g. Huang and K. S. Walton, Langmuir, 2012, 28, 16874; (d) H. Jasuja, J. Zang, D. S. Sholl and K. S. Walton, *J. Phys. Chem. C*, 2012, **116**, 23526; (e) J. B. DeCoste, G. W. Peterson, H. Jasuja, T. G. Glover, Y.-g. Huang and K. S. Walton, *J. Mater. Chem. A*, 2013, **1**, 5642.

16 J. Liu, Y. Wang, A. I. Benin, P. Jakubczak, R. R. Willis and M. D. LeVan, *Langmuir*, 2010, **26**, 14301.

17 E. Soubeyrand-Lenoir, C. Vagner, J.W. Yoon, P. Bazin, F. Ragon, Y. K. Hwang, C. Serre, J.-S. Chang and P. L. Llewellyn, *J. Am. Chem. Soc.*, 2012, **134**, 10174.

18 H. Furukawa, F. Gándara, Y.-B. Zhang, J. Jiang, W. L. Queen, M. R. Hudson and O. M. Yahgi, *J. Am. Chem. Soc.*, 2014, **136**, 4369.

19 I. A. Ibarra, S. Yang, X. Lin, A. J. Blake, P. J. Rizkallan, H. Nowell, D. R. Allan, N. R. Champness, P. Hubberstey and M. Schröder, *Chem. Commun.*, 2011, **47**, 8304.

20 I. A. Ibarra, K. E. Tan, V. M. Lynch and S. M. Humphrey, *Dalton Trans.*, 2012, **41**, 3920.

21 M. R. Gonzalez, J. H. González-Estefan, H. A. Lara-García, P. Sánchez-Camacho, E. I. Basaldella, H. Pfeiffer and I. A. Ibarra, *New J. Chem.*, 2015, **39**, 2400.

22 G. E. Cmarik, M. Kim, S. M. Cohen and K. S. Walton, *Langmuir*, 2012, **28**, 15613.

23 (a) E. Haldoupis, S. Nair and D. S. Sholl, *J. Am. Chem. Soc.*, 2012, **134**, 4313; (b) Y.-S. Bae, O. K. Farha, J. T. Hupp and R. Q. Snurr, *J. Mater. Chem.*, 2009, **19**, 2131.

24 I. P. O'koye, M. Benham and K. M. Thomas, *Langmuir*, 1997, **13**, 4054.

25 N. L. Ho, F. Porcheron and R. J.-M. Pellenq, *Langmuir*, 2010, **26**, 13287.

Inorganic Chemistry Frontiers Accepted Manuscript

This journal is © The Royal Society of Chemistry 2012